

Modeling Trace Gases in Hydrocarbon Seep Bubbles. Application to Marine Hydrocarbon Seeps in the Santa Barbara Channel

Ira Leifer¹ and Jordan Clark²

1 - Chemical Engineering Department and Marine Sciences Department, University of California, Santa Barbara, Santa Barbara, Calif. 93106-5080 USA, e - mail: ira.leifer@bubbleology.com

2 - Geological Sciences Department, University of California, Santa Barbara, Santa Barbara, Calif. 93106-5080 USA, e - mail: clark@magic.geol.ucsb.edu

Abstract

Evaluating the importance of natural marine hydrocarbon seeps to global methane budgets requires correctly predicting the gas fraction lost by the seep bubbles during transit through the water column. In the Santa Barbara Channel, California, three widely differing seeps (depth, flux, oiliness) were visited and observations were made of seep gas partial pressures, P_i , near the surface for alkanes to $n = 5$ (pentane) as well as major atmospheric gases, and upwelling flows. It was found that alkane P_i decreased exponentially with alkane diffusivity. Seabed seep gas was available for one seep, and exhibited the same trend. For alkanes heavier than methane, the ratio of the surface to sea floor mole fraction showed a linear enhancement with increasing alkane number. Methane behaved differently because the water column became saturated.

A numerical model was developed to study the sensitivity to environmental parameters of the bubble transport of seep gas to the surface. It was found that seep gas transport is highly sensitive to both upwelling flows, dissolved gas concentrations, bubble surface cleanliness, and bubble size. The model predicted that upwelling flows were increased bubble survivability and transport to the surface. It was also predicted that dissolved methane concentrations higher than 0.01 atm increased bubble survivability. When applied to simulating alkanes, the studies showed that only a narrow range in bubble size could explain the observed alkane enhancements. Thus model predictions were in agreement with the observation that a wide size range of bubbles was not observed at the sea surface.

1.0 Introduction

Natural marine hydrocarbon seeps create a unique bio-geochemical and fluid dynamical environment not easily reproducible in the laboratory. Many of the unique seep conditions are a result of the presence of rising bubbles. Bubbles exchange gas with the surrounding fluid [1], introduce turbulence [2], induce bulk fluid motions [3] [4], and efficiently transport oil and particles [5]. Evidence of several of these aspects has been provided by investigations of marine hydrocarbon seeps in the Santa Barbara Channel, CA [6]. However, the myriad processes due to bubble-bubble, fluid-bubble, and bubble-fluid interactions are at best poorly understood - for a review see *Jakobsen et al.* [7]. Even more critical, many of the basic parameterizations for the behavior of individual bubbles under seep conditions (i.e., oil, oceanic surfactants, diverse temperatures) remain unquantified. Even in the absence of detailed measurements of environmental conditions and parameterizations, numerical modeling, and in particular sensitivity studies, can play an important role in data interpretation [8]. In this regards, a valuable method for the constraint of numerical seep-bubble modeling is the simulation and measurement of trace gases. Trace gases are defined for this work as having a low partial pressure or aqueous concentration (<10% relative to total pressure or saturation) and therefore do not affect the bubble size. From the behavior of trace gases in seep

gas, conclusions can be inferred about bubble-mediated transport of seep gases including dissolution (i.e., gas transfer) into the ocean.

2.0 Field observations

2.1 Study location

Located close to the University of California, Santa Barbara, the northern margin of the Santa Barbara Channel (SBC) contains one of the most active areas of natural hydrocarbon seepage in the world. The most concentrated area of seepage is found in moderately shallow water (20 - 100 m) about 3 km offshore of Coal Oil Point, CA. It was estimated that there are more than 1000 seep vents in this seep field which continually emit both oil and gas [9]. Currently it is estimated that circa $1.7 \times 10^5 \text{ m}^3 \text{ day}^{-1}$ ($5 \times 10^6 \text{ ft}^3 \text{ day}^{-1}$) of gas is emitted to the atmosphere from these seeps [10], with equivalent amounts injected into the coastal ocean [11]. The gas consists of methane (CH_4), ethane, and other organics, grouped together as reactive organic gases (ROG). Oil discharge estimates range between 40 and 200 barrels per day [10].

2.2 Field observations

To characterize the seep environment, dissolved gases, bubble gas composition, and fluid motions were measured at three seeps of different sizes and depths, La Goleta Seep (LGS), Thor CP Seep (TCS), and Seep

Tent Seep (STS). Attributes and locations, major gas observations, and trace gas observations are presented in Tables 1, 2, and 3. At each seep, water and bubble gas samples were collected in the fluid and in the rising bubble plume at the surface. These samples were analyzed for carbon dioxide (CO₂), oxygen (O₂), nitrogen (N₂), CH₄, and higher n-alkanes to $n = 5$ (Table 2). The sea floor gas composition was estimated from measurements collected between 1982 and 1996 at the Seep Tents. For a discussion of the Seep Tents see *Rintoul* [12]; *Boles et al.* [13]. Gas composition was analyzed using standard gas chromatography techniques (Zymax Forensics, San Luis Obispo, Ca). Fluid motions were studied by tracing the movement of dye released into the column of rising bubbles and water.

Observations showed that in the rising bubbly plumes, the water possessed significant upward velocities. Thus seeps act as "vertical pumps" raising cooler, deeper water (and potentially nutrients) to the surface. The thermal signature of this phenomenon has been observed [14]. The upwelling flow generated a surface divergent flow, and thus by continuity, upward entrainment throughout the water column. The upwelling flow caused bubbles to rise faster than their stagnant-fluid rise velocity, thereby decreasing the bubbles' subsurface lifetime (enhancing transport to the surface [8] [*Leifer and Patro*, 2001]). After diverging at the surface, the cooler, denser, water sinks, entraining surface water, including oils and other substances transported to the surface by the rising bubbles [6].

Quantitative bubble observations were unavailable; however, several visual observations were made. Bubbles at the surface spanned a narrow size range, typically from circa 2 mm diameter to 1 cm. Significantly smaller bubbles were observed at STS where the upwelling flow was strongest. Also, observations of bubble motions were used to estimate likely surface cleanliness. Since large seep bubbles were observed to oscillate, this suggests that they were not highly contaminated. Furthermore, close visual observation of the larger bubbles showed a white patch, presumably oil, underneath the bubble.

An important observations was that the aqueous CH₄ concentration, C_{MET} , was supersaturated with respect to the bubble-partial CH₄ pressure, P_{MET} , in two seeps (see Table 2, STS and LGS). Values of C_{MET} for all three seeps were larger by 4 or 5 orders of magnitude than reported seep field values [11], and 9 to 10 orders of magnitude larger than background oceanic C_{MET} values (e.g., [15]; [16]). For LGS, methane supersaturation was 15% suggesting an oceanic equilibration time of only 3 s (based on hydrostatic pressure, V_{up} of 30 cm s⁻¹, and assuming no mixing between the ocean and bubble fluid).

Partial pressures for the alkane series to pentane were also determined for the bubbles (dissolved alkane concentrations were not determined). In all cases alkane partial pressure decreased with alkane number, n . At STS a comparison between seafloor and surface bubble composition showed that the lighter alkanes (ethane and butane) decreased by about 50% and that the higher alkanes decreased significantly less. Overall, during their rise, bubbles became enriched in the higher alkanes relative to the lower alkanes. This observation can be understood with respect to the process of bubble-mediated gas exchange. As a seep gas bubble rises, it exchanges gas with the surrounding water (seep gases outflow and atmospheric gases inflow). Since this is a diffusive process, the heavier alkanes with lower diffusivity, D , exchange slower, and as a result, bubbles become enriched with these gases.

Table 1. Natural hydrocarbon seeps visited. Locations are at 119°W, 34°N. TCS - Thor CP, LGS - La Goleta Seep, STS - Seep Tent Seep.

Name	Location (Lat. , Lon.)	Depth (m)	Area (m ²)	V_{up} m s ⁻¹	Relative Activity
TCS	52.442', 23.650'	20	2	-	Low
LGS	51.183', 22.500'	70	25	0.3	Active
STS	53.350', 23.050'	70	700	>1	Extreme

V_{up} is the upwelling velocity.

The gas exchange process has been long studied, e.g., [17]; [18]. For flat, clean surfaces (i.e., the ocean surface in the absence of slicks, or large bubbles) gas exchange efficiency varies as $D^{0.5}$ [19]. Unlike the ocean, due to their finite volume, bubbles can equilibrate with the surrounding water, causing gas exchange to vary volumetrically, i.e., by solubility. Also due to their finite volume, when a bubble dissolves it forces all internal gases into the water. In such a case, gas exchange depends upon the mole fraction of the gas in the bubble and bubble exchange has neither a solubility nor diffusivity dependency. In reality, all three processes occur to varying extent in a bubble stream. Smaller bubbles will dissolve, while intermediate size bubbles may partially dissolve. Larger bubbles grow, and while some gases may achieve near equilibrium for bubbles smaller than some size, other gases in larger bubbles may not. Thus examining the diffusivity and solubility dependency of bubble gas exchange for the bubble stream highlights which bubble sizes and processes are most important. In fact, these dependencies present a powerful constraint for bubble gas exchange modeling, and can be used in conjunction with modeling sensitivity studies to draw conclusions about the fate of seep gas.

The alkane mole fraction at the surface divided by the mole fraction at the seafloor for STS are shown in

Table 2. Summary of major gases bubble partial pressures and dissolved concentrations. *STS₂* is STS corrected to 2 m for comparison with other seeps. *STSB* is STS at the sea bed.

Seep	<i>z</i> (m)	<i>P</i> (O ₂) mbar	<i>P</i> (N ₂) mbar	<i>P</i> (CH ₄) mbar	<i>C</i> _{MET} μMol/l	<i>H</i> <i>C</i> _{MET} mbar
STS	1	85	251	691	1000	860
<i>STS₂</i>	2	93	274	754	-	-
LGS	2	105	339	700	1200	810
TCS	2	75	203	758	260	190
		%		%	%	
STS	1	7.69	22.8	62.8	1000	860
STSB	70	0.14	0.79	87.5	-	-

z is sample depth, *P* is partial pressure, *C* is concentration, MET is CH₄, and *H* is the Henry's Law Constant for 12°C.

Fig. 1. With the exception of CH₄, the ratio increased with alkane size, showing a strong dependency on either solubility or diffusivity, since both alkane solubility and diffusivity increase with *n*. The behavior of CH₄ can be explained in terms of bubble gas transfer and is discussed in Section 3.0.

2.3 Discussion

At the surface, CH₄ was saturated within the plume. Since the seep bubbles are the primary CH₄ source, saturation implies that bubble gas transfer, which causes CH₄ to outflow the bubbles, is more efficient than CH₄ diffusion and advection from the bubble stream to the bulk ocean. Thus bubbles cause the aqueous CH₄ concentration to be close to equilibrium with the bubble CH₄ partial pressure. Observations showed that *C*_{MET} was supersaturated with respect to the bubble partial pressure, and this is a direct result of the upwelling flow. At greater depth the hydrostatic pressure is larger, and thus the saturation pressure is larger. Therefore the CH₄ supersaturation represents bubble outflow in deeper water lifted to the surface by the upwelling flow. Another impact of marine seepage is that O₂ and N₂ inflow into the bubbles thereby undersaturating the bubble plume with respect to bulk ocean *C*_{O₂} and *C*_{N₂} - i.e., seep bubbles strip the dissolved air gases from the water at the same time that they outflow seep gases. Because dissolved gas concentrations are less, air inflow into the bubbles is also reduced, or alternatively, bubble dissolution is increased and thus CH₄ transport to the surface decreased (larger bubbles will dissolve). In fact, as discussed below, bubble gas transport is strongly sensitive to deviations of the dissolved major gas concentrations.

Table 3. Summary of trace gas bubble observations at sample depths listed in Table 2. For STS units are % mole fraction.

Seep	<i>P</i> (C ₂ H ₆) mbar	<i>P</i> (C ₃ H ₈) mbar	<i>P</i> (C ₄ H ₁₀) mbar	<i>P</i> (C ₅ H ₁₂) mbar
STS	25.6	19.6	4.54	2.93
<i>STS₂</i>	27.9	21.4	4.95	3.19
LGS	20.6	16.3	5.14	2.98
TCS	14.6	17.7	5.95	4.54
	%		%	%
STS	2.33	1.78	0.41	0.27
STSB	5.09	3.07	0.43	0.24

P is partial pressure.

The upwelling flow also affects bubble dissolution. By decreasing the subsurface lifetime, an upwelling flow allows smaller bubbles to survive to the surface that would have dissolved otherwise. This is one explanation of the presence of smaller bubbles at STS than LGS since in both cases the water was saturated.

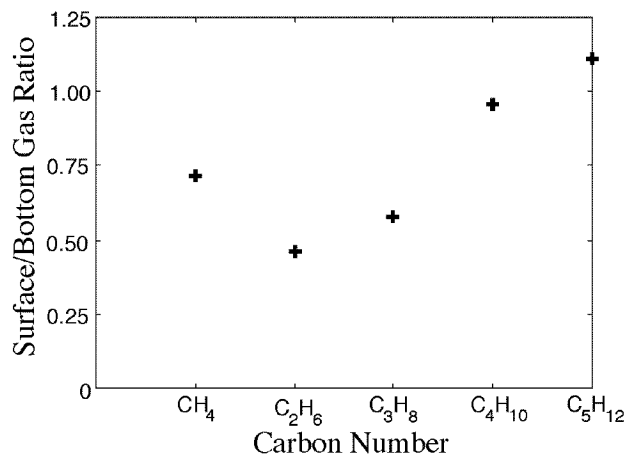


Fig. 1 Surface to bottom ratio of n-alkane mole fractions in gas phase for STS.

3.0 Bubble-mediated seep gas modeling

3.1. Model

Bubble-mediated seep gas modeling can be used to answer several types of questions. Given a complete set of observations and a validated model, gas transport to the surface and into the water column for different seeps under different conditions can be predicted. However, validated models do not exist [20], nor does sufficient observational data exist for model validation. In the

absence of a complete data set, bubble modeling can still be used to draw conclusions about the importance of different bubble plume processes. Modeling can also be used to conduct sensitivity studies indicating which future measurements are most needed. For a detailed review of issues regarding bubble seep modeling see *Leifer and Patro* [21].

A bubble-mediated gas transfer model [21] was used to investigate the effect of dissolved methane and upwelling flows on methane transport to the surface for the seeps described above. The model was also used to investigate n-alkane transport to the surface. The model solves the coupled differential equations that describe the change in bubble mass, radius, pressure, and depth as a bubble rises, exchanges gas and grows due to gas exchange and changing hydrostatic pressure. To solve the equations, a third-fourth order adaptive step-size Runge-Kutta method was used. The bubble gas transfer rate, k_B , and rise velocity, V_B , are parameterized, and the upwelling flow is either an observed or assumed value. Values of D and H are from [22] for seawater except for n-alkanes. Published values of D and H for most alkanes in seawater are unavailable and freshwater values from [23] for 15°C were used.

For this study the model used the clean V_B parameterization of [24]. The model was run for LGS surface conditions for three different bubble contamination cases, "all clean", "all dirty", and "varying" at 15°C. Contamination is by surface active substances in the ocean water, which diffuse to and are adsorbed onto the bubble surface where they retard the bubble surface mobility through a process called the Marangoni effect. Contaminated bubbles rise slower and transfer gas slower [8]. While small bubbles are very likely to be dirty, seep observations of bubble oscillations suggest the interfaces of large ($r > 1000 \mu\text{m}$) bubbles are hydrodynamically clean. In the "varying" surfactant case, small bubbles were dirty and large clean with a transition at $700 \mu\text{m}$. Bubbles were initialized with STS sea floor composition.

3.2. Sensitivity studies

3.2.1 Dissolved CH_4

The sensitivity study for "all clean" bubbles and $V_{up} = 30 \text{ cm s}^{-1}$ with varying aqueous C_{MET} is shown in Fig. 2a. Fig. 2a shows the predicted CH_4 fraction in the bubble at the surface, the remainder having been lost to the water. Also shown is the observed CH_4 fraction at the surface, indicated by the horizontal dashed line. As can be seen, there is little difference when the aqueous CH_4 concentration is equivalent to CH_4 partial pressures of 0.01 Atm or 0.1 Atm (calculated by HC_{MET} , which is the pressure that a gas in contact with the liquid would be in if it was in equilibrium). However, if the water column CH_4 concentration is

larger (e.g., $HC_{MET} = 1 \text{ Atm}$) smaller bubble survivability is significantly increased and larger bubbles transport significantly more CH_4 to the atmosphere.

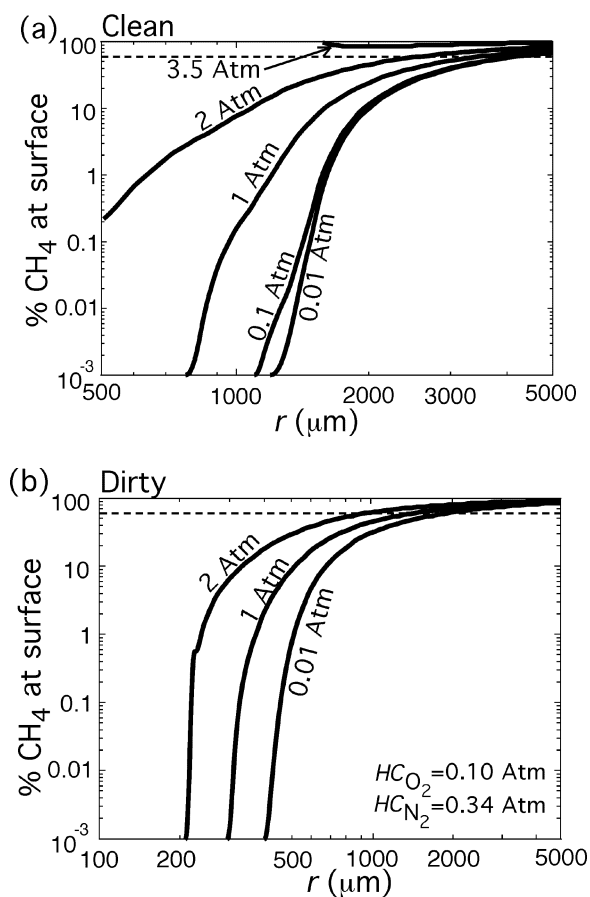


Fig. 2 Sensitivity study of importance of bubble cleanliness and C_{MET} , to fraction of initial CH_4 transported to the surface for different bubble radii, r . Dissolved O_2 and N_2 (HC_{O_2} , HC_{N_2}) on (b). Dashed line indicates observed % CH_4 at surface. Note: different lower limit to x axis.

The simulation for $HC_{MET} = 1 \text{ Atm}$ showed that if the emitted bubbles were monodisperse (i.e., a single size), then the observed surface CH_4 fraction of 70%, requires 2500- μm bubbles at the seafloor. The model also predicted that 2500- μm bubbles roughly double in size as they rise to the surface. Because bubbles this large were not commonly observed at the surface, dissolved subsurface plume CH_4 concentrations at greater depth must have been greater than 1 Atm. Only surface observations of aqueous CH_4 were available, but due to hydrostatic pressure, it is reasonable that dissolved CH_4 concentrations were much larger at

greater depth. For example, if HC_{MET} was 2 Atm, many bubbles that would have dissolved at lower aqueous CH_4 do not, while if HC_{MET} was 3.5 Atm (equivalent to hydrostatic pressure for 35 m, i.e., 1/2 the seep depth), small bubbles rapidly grow or effervesce. Thus higher aqueous CH_4 allows bubbles with smaller initial radius to explain the observed surface CH_4 fraction. However, the higher aqueous CH_4 causes more rapid bubble growth. As a result, the model predicts that bubbles arrive at the surface larger than observed. Therefore additional processes must be more important than higher aqueous CH_4 .

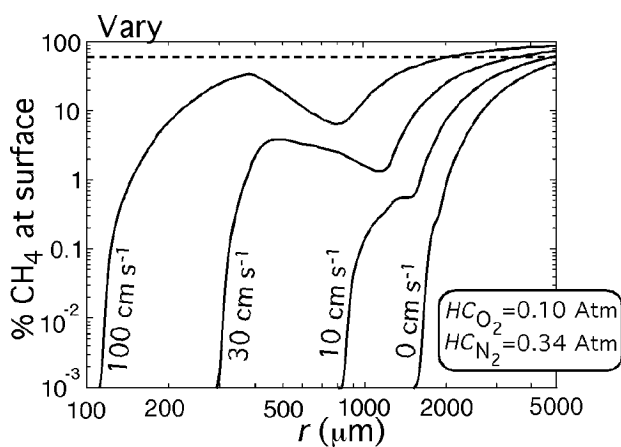


Fig. 3 Sensitivity study of importance of upwelling flow to CH_4 transport to the surface for different bubble radii, r , for the "varying surfactant" case.

3.2.2 Surface cleanliness

One dubious assumption in the simulations shown in Fig. 2a is that small bubbles are clean, particularly given the observation that when bubbles burst at the surface small oil slicks formed. The sensitivity studies were repeated for completely contaminated bubbles, shown in Fig. 2b (note the different r scale from Fig. 2a). For dirty bubbles, transport to the surface is greater and much smaller bubbles reach the surface. Also, sensitivity to dissolved CH_4 is reduced. For contaminated bubbles and $HC_{MET} = 1$ Atm, 800- μ m bubbles (which do not grow appreciably) can explain the observed surface P_{MET} . And, in fact, bubbles of this size were observed at the surface.

These sensitivity studies illustrate that bubble surface cleanliness is important. Bubble cleanliness can be determined in the laboratory or field by measuring the rise speed, and comparing with theoretical clean and dirty bubble rise speeds. Unfortunately rise speeds were not measured. Laboratory studies of bubbles in collected seawater and salt marsh water showed that small bubbles

were dirty and large bubbles were clean, as determined by their rise velocity [25]. A transition was observed at circa 800 μ m. This behavior arose because surfactants pool in a stagnant cap at the downstream hemisphere [26]. If the cap extends far enough, it affects the bubble hydrodynamics. Since the flow is stronger for larger bubbles, the angular extent of the cap decreases with size (all other things being equal). Although this model is not appropriate for all surfactants, it has been confirmed for industrial surfactants [27], and describes the observations of *Patro et al.* [25], although oily bubble observations are unavailable. Nevertheless it is unlikely that seep bubbles were all either dirty or clean. Instead small bubbles were probably hydrodynamically dirty while large bubbles were hydrodynamically clean.

Several visual observations suggest that large bubbles were clean while smaller bubbles were dirty. When bubbles are completely contaminated, bubble shape and trajectory oscillations are highly damped [24]. Since large seep bubbles were observed to oscillate, this suggests they were not highly contaminated. Furthermore, close visual observation of the larger bubbles showed a white patch, presumably oil, underneath the bubble. Thus large bubbles were probably clean, while small bubbles were dirty.

3.2.3 Upwelling Flow

In addition to dissolved CH_4 and surface cleanliness, bubble gas exchange is sensitive to upwelling flows. Upwelling flows decrease a bubble's subsurface lifetime and increase the rate that the hydrostatic pressure decreases as the bubbles rise. A sensitivity study to upwelling flow for the case of "varying surfactant" contamination is shown in Fig. 3. The k_B and V_B parameterizations were set to transition from dirty to clean at $r = 500$ μ m with a transition width of 200 μ m, based on the parameterization of [28], in rough agreement with bubble V_B observations in seawater [25]. However, it is possible that for oily bubbles the transition is at larger r . C_{MET} methane was 0.8 Atm. The effect of the varying surfactant contamination, seen as the "S" shape of the curves, is to increase k_B and V_B for larger bubbles. While the increase in k_B decreases CH_4 transport to the surface (more dissolution), the increase in V_B increases transport to the surface by decreasing subsurface lifetime. It is the interplay between these two processes that generates the "S" shape. Even a small upwelling flow (10 $cm\ s^{-1}$) has quite a strong effect on CH_4 transport to the surface. However, a significantly larger V_{up} than observed for LGS is required to generate the observed P_{MET} (indicated by dashed line) but this also would allow bubbles smaller than observed to survive to the surface. Interestingly, only at STS where V_{up} was larger than

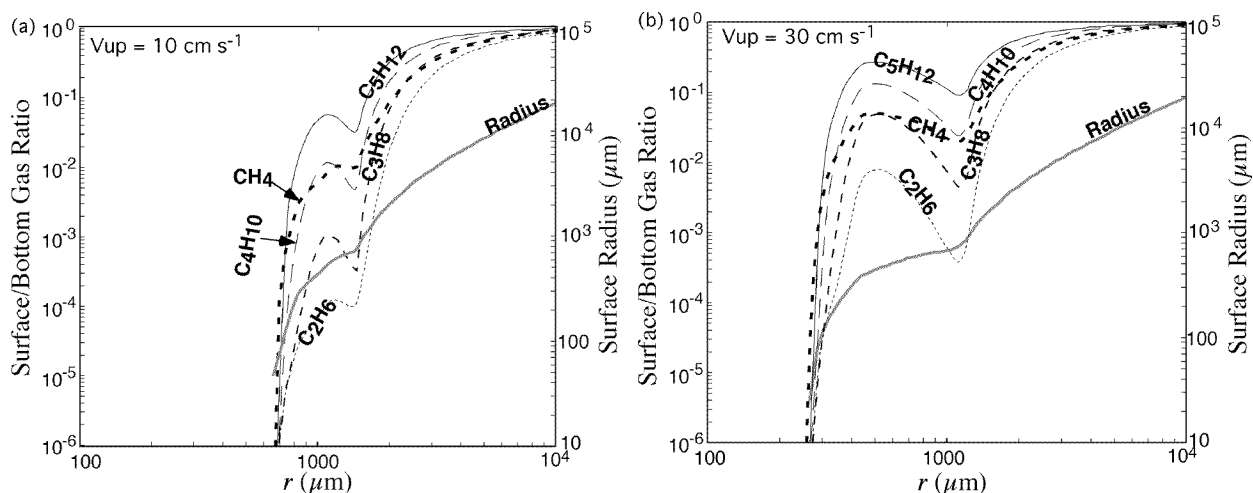


Fig. 4 Sensitivity results showing predicted ratio of bubble alkane molar content at surface versus sea bed as a function of bubble radius, r for (a) upwelling flow, V_{up} , of 10 cm s^{-1} , and (b) V_{up} of 30 cm s^{-1} . Also shown is the surface r on the right vertical axis. Alkane and surface r labeled on plot.

100 cm s^{-1} were bubbles as small as $200 \mu\text{m}$ observed. Thus while there was a strong sensitivity to upwelling flow for varying surfactant, it was unable to produce the observed surface CH_4 fraction. However, if one took the dirty curves for bubbles smaller than $500 \mu\text{m}$ and assumed that the dirty-clean transition was at larger r , for example $1000 \mu\text{m}$, a V_{up} of 30 cm s^{-1} or greater could explain observations.

3.3. Trace Gases

Two studies of the sensitivity of heavier alkane gas transport to V_{up} were conducted for $H_{C_{MET}} = 0.9 \text{ Atm}$ and are shown in Fig. 4. The figure shows the ratio of the moles of each alkane at the surface to the bottom, and thus is for comparison with Fig. 1. Also shown (left axis) is the bubble r at the surface. Thus for $V_{up} = 10 \text{ cm s}^{-1}$ (Fig. 4a), a $2000\text{-}\mu\text{m}$ bubble reaches the surface with $r \sim 2000 \mu\text{m}$, while a $900\text{-}\mu\text{m}$ bubble reaches the surface with $r \sim 300 \mu\text{m}$. For all bubbles, the ratio increased with alkane number, except for CH_4 , and this is due to saturation of the water column with CH_4 . Yet the relative enhancement of heavier versus lighter alkanes is greatest for bubbles that dissolved slightly and least for the largest bubbles (which grow). For the largest bubbles this results from the large volume, i.e., during their ascent to the surface, the bubbles' total molar content changes little due to gas exchange. In contrast, when a bubble dissolves, as indicated by the decrease in CH_4 at circa $800 \mu\text{m}$, all gases are equally forced from the bubble, and thus there is little difference in the relative enhancement of heavier and lighter alkanes. As a result, there is a narrow size band which can explain the observed enhancement. In fact, circa

$3000\text{-}\mu\text{m}$ bubbles produce a relative enhancement of 2 for pentane versus ethane. For these conditions, bubbles with initial r circa $3000 \mu\text{m}$ must be responsible for most of the gas transport in the plume. These bubbles do not change size appreciably, and thus are in agreement with the observed bubble sizes for La Goleta Seep. In the model, bubbles smaller than circa $1000 \mu\text{m}$ dissolved too much (i.e., were too small at the surface), while bubbles larger than $5000 \mu\text{m}$ grew too large. Thus the emitted distribution must also be fairly narrow.

Not surprisingly, for different ambient conditions, the conclusions about the initial distribution changes. If $V_{up} = 30 \text{ cm s}^{-1}$, smaller bubbles over a wider range, from 500 to $2000 \mu\text{m}$ can now explain alkane observations. Since dissolution is less, a wider size range of bubbles can satisfy the observed surface bubble sizes. This results from the stronger upwelling flow decreasing the subsurface time for bubble dissolution. Due to the upwelling flow, the bubble size where the initial r is the same as the surface r has decreased slightly to circa $2500 \mu\text{m}$.

4.0 Conclusions

Observations of natural marine hydrocarbon seeps in the Santa Barbara Channel show CH_4 saturation in the bubble plume. Sensitivity studies showed that CH_4 transport to the surface is highly sensitive to significant dissolved CH_4 concentrations ($H_{C_{MET}} > 0.1 \text{ Atm}$). Simulations of all bubbles as clean or dirty were less convincing, than a varying surfactant simulation where small bubbles were dirty and large bubbles clean. Observations also showed strong upwelling flows in the seeps. Sensitivity studies also showed a strong sensitivity to upwelling flows.

Alkane partial pressures to $n = 5$ were observed in seep bubbles. The ratio of the surface to bottom alkane fraction was found to show an enhancement that increased approximately linearly with n for $n > 2$, the exception being CH_4 which was saturated in the water. Alkane sensitivity studies showed that only a narrow r range could explain the observed alkane enhancements. This size range was narrowed even further when predicted surface bubble size was compared with surface bubble observations.

This paper has shown that alkane measurements can constrain bubble models and allow conclusions to be drawn about environmental conditions in the water column.

Acknowledgments. The support of the University of California Energy Institute and the Department of Energy, Grant No. DE-F603-85ER-13314 is gratefully acknowledged. We would also like to acknowledge the work of Shane Anderson and Dave Farrar for field work. This is contribution 370-101TC of the Institute for Crustal Studies at the University of California, Santa Barbara.

References

- [1] Keeling, R.F. 1993. On the role of large bubbles in air-sea gas exchange and supersaturation in the ocean. *J. Mar. Res.* 51, 237-271.
- [2] Monahan, E.C., and M.C. Spillane, 1984. The role of oceanic whitecaps in air-sea gas exchange. In *Gas Transfer at Water Surfaces*. Eds. W. Brutsaert and G. H. Jirka. D. Reidel Pub. Co. Dordrecht, Holland. 495-503.
- [3] Asher, W.E., L.M. Karle, and B.J. Higgins, 1997. On the difference between bubble-mediated air-water transfer in freshwater and sea water. *J. Mar. Res.* 55(5), 1-34.
- [4] Chen, R.C., J. Reese, and L.-S. Fan, 1994. Flow structure in a three-dimensional bubble column and three-phase fluidized bed. *AIChE J.* 40(7), 1093-1104.
- [5] Blanchard, D.C., 1989. The size and height to which jet drops are ejected from bursting bubbles in sea water. *J. Geophys. Res.* 94, 10 999-11 002.
- [6] Leifer, I., J.F. Clark, and R.F. Chen, 2000. Modifications of the local environment by natural hydrocarbon seeps. *Geophys. Res. Lett.*, 27(22), 3711-3714.
- [7] Jakobsen, H.A., B.H. Sannaes, S. Grevskott, and H.F. Svendsen, 1997. Modeling of vertical bubble-driven flows. *Ind. Eng. Chem. Res.* 36, 4052-4074.
- [8] Leifer I., and R. Patro, 2001. The bubble mechanism for transport of methane from the shallow sea bed to the surface : A review and sensitivity study. *Accepted to Cont. Shelf Res.*
- [9] Fischer, P.J., 1978. Oil and tar seeps, Santa Barbara basin, California, in California offshore gas, oil, and tar seeps, California State Lands Commission Staff Report, Sacramento, California, p. 1-62.
- [10] Hornafius, J.S., D. Quigley, and B.P. Luyendyk, 1999. The world's most spectacular marine hydrocarbon seeps (Coal Oil Point, Santa Barbara Channel, California): Quantification of emissions, *J. Geophys. Res.*, 104, 20 703-20 711.
- [11] Clark, J.F., L. Washburn, J.S. Hornafius, B.P. Luyendyk, 2000. Dissolved hydrocarbon flux from natural marine seeps to the Southern California Bight, *J. Geophys. Res.*, 105, 11,509-11,522.
- [12] Rintoul, W. 1982. ARCO caps Santa Barbara Channel seep, *Pac. Oil World* 74, 6-9.
- [13] Boles, J.R., J.F. Clark, I. Leifer, and L. Washburn, 2001. Temporal variation in natural hydrocarbon flux from natural marine seeps to the Southern California Bight, *submitted to J. Geophys. Res.*
- [14] Washburn, L., C. Johnson, S.S. Gotschalk, and E.T. Eglund, 2000. A gas-capture buoy for direct measurement of bubbling gas flux in oceans and lakes. *submitted to J. Atmos. Ocean. Tech.*
- [15] Conrad, R., and W. Seiler, 1988. Methane and hydrogen in sea water (Atlantic ocean). *Deep Sea Res.* 12, 1903-1917.
- [16] Cynar, F.J. and A.A. Yayanos, 1992. The distribution of methane in the upper waters of the Southern California Bight, *J. Geophys. Res.* 97, 11 269-11 285.
- [17] Liss, P.S., 1973. Process of gas exchange across an air-water interface. *Deep Sea Res.* 20, 221-238.
- [18] De Leeuw, G., G.J. Kunz, G. Caulliez, L. Jaouen, S. Badulin, D.K. Woolf, P. Bowyer, I. Leifer, P. Nightingale, M. Liddicoat, T.S. Rhee, M.O. Andreae, S.E. Larsen, F.Aa Hansen, and S. Lund, 2001. LUMINY - An Overview, in *Gas Transfer and Water Surfaces*, Eds. E.S. Salzman, M. Donelan, W. Drennan, and R. Wanninkhof, American Geophysical Union, *accepted*.
- [19] Jähne B., K.O. Münnich, R. Börsinger, A. Dutzi, W. Huber, and P. Lißner, 1987. On the parameters influencing air-water gas exchange. *J. Geophys. Res.* 92(C2), 1937-1949.
- [20] Yapa, P.D., and L. Zheng, 1997. Simulation of oil spills from underwater accidents I: Model development. *J. Hydraul. Res.*, 35(5), 673 - 687.
- [21] Leifer I., and R. Patro, 2001. The bubble mechanism for methane transport from the shallow sea bed to the surface: A review and sensitivity study. *Cont. Shelf Res.* *accepted*.
- [22] Wanninkhof, R, 1992. Relationship between wind speed and gas exchange over the ocean. *J. Geophys. Res.* 97 C5, 7373-7382.
- [23] Sander, R., 2000. Henry's Law Constants in NIST Chemistry WebBook, NIST Standard Reference Database, Number 69, Eds. W.G. Mallard and P.J. Linstrom, National Institute of Standards and Technology, Gaithersburg MD (<http://webbook.nist.gov>).
- [24] Leifer I., Patro, R., and P. Bowyer, 2000. A study on the temperature variation of rise velocity for large clean bubbles. *J. Atm. and Ocean. Tech.*, 17(10), 1392-1402.
- [25] Patro, R., I. Leifer, and P. Bowyer, 2001. Better bubble process modeling : Improved bubble hydrodynamics parameterisation. In *Gas Transfer at Water Surfaces*,

- Eds. M. Donelan, W. Drennan, E.S. Salzman, and R. Wanninkhof, American Geophysical Union, *accepted*.
- [26] Sadhal S. and R.E. Johnson, 1983. Stoke's flow past bubbles and drops partially coated with thin films. *J. Fluid Mech.* **126**, 237-250.
- [27] Fdhila, R.B., and P.C. Duineveld, 1996. The effect of surfactants on the rise of a spherical bubble at high Reynolds and Peclet numbers. *Phys. Fluids* **8**, 310-321.
- [28] Tsuchiya, K., H. Mikasa, and T. Saito, 1997. Absorption dynamics of CO₂ bubbles in a pressurized liquid flowing downward and its simulation in seawater. *Chem. Eng. Sci.* **52(21/22)**, 4119-4126.